

# Photoelectron Spin-Polarisation Spectroscopy in the $5s5p^2$ -Autoionisation Region of Indium

M. Müller, N. Böwering, F. Schäfers\* and U. Heinzmann

Fakultät für Physik der Universität Bielefeld, D-4800 Bielefeld, Federal Republic of Germany; Fritz-Haber-Institut der MPG, D-1000 Berlin 33, Federal Republic of Germany; \*BESSY, Lentzeallee 100, D-1000 Berlin 33, Federal Republic of Germany

Received July 16, 1989; accepted September 14, 1989

## Abstract

Photoelectron spin-polarisation measurements of  $\text{In}(5s^25p)^2P_{1/2}$  were performed in the autoionisation region of the  $5s5p^2$ -configuration using monochromatic circularly polarised synchrotron radiation at the electron storage ring BESSY. The autoionising levels are analysed in terms of partial cross section, dipole matrix elements and phase-shift differences. In addition the measured photoelectron spin-polarisation data were used for an independent check for the assignments of the autoionising levels.

## 1. Introduction

The technique of angle- and spin-resolved photoelectron spectroscopy has been shown to be a useful method for analysing the dynamics of the photoionisation process in terms of “experimental” dipole matrix elements and phase-shift differences (Heinzmann [1, 2], Schäfers *et al.* [3], Schönhense *et al.* [4], Heckenkamp *et al.* [5]). By measuring the spin-polarisation vector of the photoelectrons, one obtains the three independent spin-polarisation parameters  $A$ ,  $\alpha$  and  $\xi$  describing the photoionisation process. Together with the photoionisation cross-section and the angular asymmetry parameter  $\beta$ , which are well-known in most cases, a set of five dynamical parameters is available for a complete quantum-mechanical characterization of the photoionisation process (Heinzmann [1, 2]).

This paper presents the first photoelectron spin-polarisation measurements of  $\text{In}(5s^25p)^2P_{1/2}$  in the autoionisation region above the first ionic threshold  $\text{In}^+(5s^2)^1S_0$  ( $\lambda = 214.14$  nm) in the wavelength range from 190.0 to 162.0 nm. In this range the photoionisation cross-section is strongly influenced by the atomic levels of the configuration  $\text{In}(5s5p^2)$  ( $^2S$ ,  $^2P$  and  $^2D$ ). These autoionisation resonances have been the subject of several photoabsorption experiments using conventional continuum-light sources (Garton [6], Garton *et al.* [7], Marr and Heppingstall [8], Kozlov and Startsev [9]) or synchrotron radiation (Connerade *et al.* [10]) and one experiment involving photoion spectroscopy (Karamatskos *et al.* [11]). Since the fine-structure splitting of the ground state  $\text{In}(5s^25p)^2P_{1/2,3/2}$  is  $\Delta E = 0.27$  eV both levels are thermally populated at an evaporation temperature of 1350 K. Consequently one expects two fine-structure peaks for any autoionising level (with  $J = 1/2$  or  $3/2$ ) in a photoabsorption experiment. Problems arise with regard to the  $\text{In}(5s5p^2)^2S_{1/2}$ -transitions, since all photoabsorption experiments show only one strong line at  $\lambda = 175.7$  nm. The question arises whether this line should be attributed to the  $\text{In}(5s^25p)^2P_{1/2} \rightarrow \text{In}(5s5p^2)^2S_{1/2}$  [8] transition or to  $\text{In}(5s^25p)^2P_{3/2} \rightarrow \text{In}(5s5p^2)^2S_{1/2}$  [6]. Garton *et al.* [7] tried to solve this question using a shock-tube technique, heating indium up to 5300–6300 K. Their

absorption spectra show a *weak diffuse absorption feature* at  $\lambda \sim 183$  nm. They interpreted this extremely weak structure to the  $^2P_{3/2} \rightarrow ^2S_{1/2}$  transition. Consequently, the 175.7 nm line should be assigned to the  $^2P_{1/2} \rightarrow ^2S_{1/2}$  transition.

Theoretical studies (Hartree-Fock-calculations) of Connerade and Baig [10] for the  $sp^2$ -configuration of the three isoelectronic sequences Ga I to Tl I supported this assignment and Karamatskos *et al.* [11] recently confirmed these HF-calculations with respect to the mixing amplitudes for several autoionising levels deduced from the measured widths of these resonances. Up to now no theoretical explanation for the extreme weakness of the  $^2P_{3/2} \rightarrow ^2S_{1/2}$  transition has been given.

A more reliable experimental check for the assignments of the autoionising levels of the  $sp^2$ -configuration from third group elements can be accomplished by photoelectron spectroscopy in connection with detection of the photoelectron spin-polarisation: By resolving the fine-structure splitting in the ground state by the use of an electron spectrometer the assignment of the line at  $\lambda = 175.7$  nm can be directly determined. Furthermore, photoelectron spin-polarisation analysis provides the  $j$ -quantum numbers of the autoionising levels as firstly demonstrated in an experiment on thallium by Heinzmann *et al.* [12]. Cherepkov [13] suggested to use this method in order to clarify the missing line problem of indium. Later Cherepkov [14] gave a prediction for the energy dependence of the spin-polarisation parameter  $A$  of In.  $A$  is the spin-polarisation of the total photoelectron flux regardless of their direction of emission using circularly polarised light (“Fano effect”, Fano [15], Heinzmann [16]). In his prediction, Cherepkov assumed that the fine-structure splitting in the ground state is not resolved in the experiment.

The object of this paper is first to give an independent experimental check for the assignments of the autoionising levels of the  $sp^2$ -configuration of In and secondly to analyse the photoionisation process in terms of dipole-matrix elements and phase-shift differences by means of the experimental data of the photoelectron spin-polarisation.

## 2. Experimental

The spin-polarised photoelectron spectroscopy was performed in an experiment with circularly polarised synchrotron radiation at the electron storage ring BESSY (Berlin). A detailed description of the experimental arrangement has been given by Heckenkamp *et al.* [5, 17].

Briefly, circularly polarised VUV synchrotron radiation, emitted out off plane, is monochromatised by a 6.5 m normal

incidence monochromator ( $\Delta\lambda = 0.5$  nm) (Schäfers *et al.* [18]) and crosses an atomic beam of indium. The reaction plane is defined by the momenta of photon and photoelectron. The photoelectrons emitted at the emission angle  $\Theta$  are energy-analysed by a hemispherical electron spectrometer (rotatable around the normal of the reaction plane) and, after two electrostatic deflections by 90 degrees, are accelerated to 100 keV and scattered on a thin gold foil of the Mott-detector for spin-polarisation analysis. Two transverse spin-polarisation components,  $A(\Theta)$  (component in the direction of the incident photon beam) and  $P_{\perp}(\Theta)$  (component perpendicular to the reaction plane), are determined simultaneously:

$$A(\Theta) = \gamma \frac{A - \alpha P_2[\cos(\Theta)]}{1 - \beta/2 \cdot P_2[\cos(\Theta)]} \quad (1a)$$

$$P_{\perp}(\Theta) = \frac{2\xi \cos(\Theta) \sin(\Theta)}{1 - \beta/2 \cdot P_2[\cos(\Theta)]} \quad (1b)$$

with  $\gamma = \pm 1 =$  helicity of light,  $P_2[\cos(\Theta)] =$  second Legendre polynomial,  $\beta =$  angular asymmetry parameter of photoelectron intensity,  $A, \xi, \alpha =$  photoelectron spin-polarisation parameters.

By measuring at the so called magic-angle  $\Theta_m = 54^\circ 44'$  (where  $P_2[\cos(\Theta)] = 0$ ) one obtains directly the spin-polarisation parameters  $A$  and  $\xi$ , whereas the third spin-polarisation parameter  $\alpha$  is determined by fitting the angular distribution of  $A(\Theta)$  according to eq. (1a).

A resistively heated high-temperature atomic-beam oven was used to evaporate Indium (purity = 99.99%) from a boron-nitride crucible with a molybdenum nozzle, heated up to 1350 K, yielding an estimated target pressure of about  $1 \times 10^{-1}$  mbar. Increasing the temperature of the atomic-beam oven from 1000 K to 1350 K resulted in a rise of the target pressure from  $6 \times 10^{-3}$  to  $1 \times 10^{-1}$  mbar; however, the photoelectron spin-polarisation parameters have been measured to be independent of the target density. So systematic errors caused by electron scattering processes can be excluded. The heating wire (0.2 mm  $\varnothing$ , Mo) is directly wound bifilarly on the boron-nitride crucible in order to compensate magnetic fields produced by the heating current (DC). Shielding with molybdenum-foils reduces the thermionic electrons to a minimum. By remeasuring some well known photoelectron spin-polarisation data of Xe( $5p^6$ ) (Heckenkamp *et al.* [5]) with heated empty atomic beam oven we checked that the compensation of the magnetic fields is sufficient.

### 3. Results and discussion

The photoionisation process of indium atoms above the first ionisation threshold (214.14 nm)  $\text{In}^+(5s^2)^1S_0$  is described by the following reaction scheme:

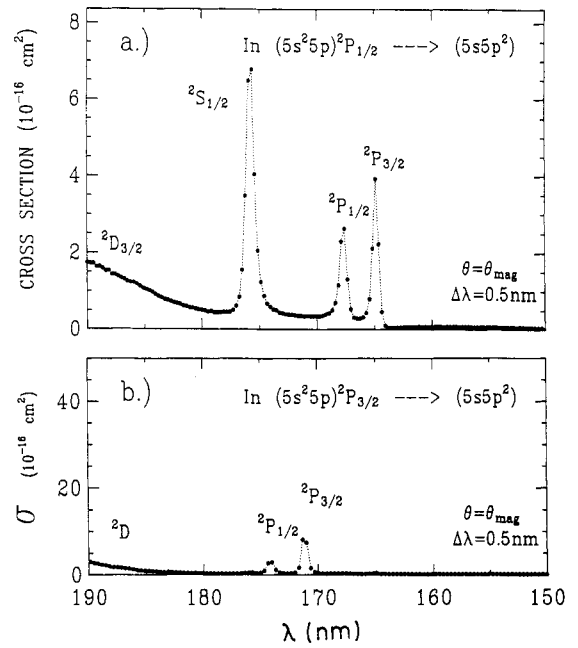
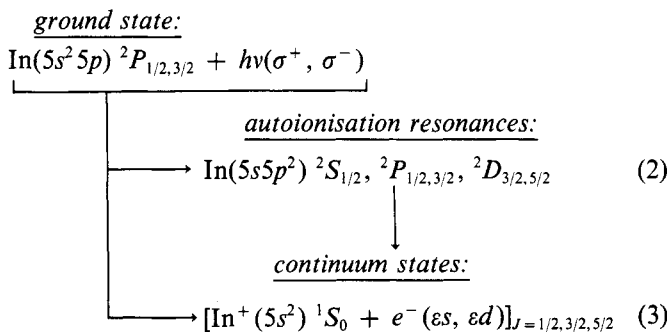


Fig. 1(a, b). Partial photoionisation cross section of  $\text{In}(5s^2 5p)$  in the autoionisation region of the  $(5s5p^2)$ -configuration for both ground states  $^2P_{1/2}$  and  $^2P_{3/2}$ . The data are determined by the measured photoelectron intensity ( $\Delta\lambda = 0.5$  nm), recorded at the magic angle ( $\Theta_m$ ) and normalized to the storage ring current, the photonflux [18] and to the different thermal population of  $\text{In}(5s^2 5p)^2P_{1/2}$  to  $^2P_{3/2}$  at the evaporation temperature of 1350 K. The absolute scaling was performed by comparison of our relative data to the absolute cross section measurement of Kozlov *et al.* [9].

The autoionising states of the  $5s5p^2$ -configuration are labelled in  $LS$ -notation. Fine-structure splitting in the ground state ( $5s^2 5p$ ) leads to a  $^2P_{1/2}$  and a  $^2P_{3/2}$  level split by  $\Delta E = 0.27$  eV. When working at oven temperatures of 1350 K, both levels are thermally populated in a ratio of:  $^2P_{1/2}/^2P_{3/2} \approx 6/1$ . By performing energy analysis of the photoelectrons one can study each transition process separately. Figure 1(a, b) shows the partial photoionisation cross-sections of indium for both ground states in the wavelength region between 190 to 150 nm as determined by the measured photoelectron intensity ( $\Delta\lambda = 0.5$  nm), recorded at the magic angle ( $\Theta_m$ ) and normalized to the photon flux (grating efficiency [18]), to the storage ring current and to the different population of  $\text{In}(5s^2 5p)^2P_{1/2}$  to  $^2P_{3/2}$  at our evaporation temperature of 1350 K. The absolute scaling was performed by comparison of our relative data to the absolute cross section of Kozlov *et al.* [9]. The assignments of the autoionisation resonances given in Figs. 1(a, b) are adopted from the Hartree-Fock calculation of Connerade *et al.* [10] and are discussed below. From the photoionisation cross-section data [Figs. 1(a, b)] it is clear that the resonance at  $\lambda = 175.7$  nm refers to the excitation of the  $^2P_{1/2}$ -ground state of indium.

In the following we examine the photoionisation process referring to the  $\text{In}(5s^2 5p)^2P_{1/2}$  ground state. The final states (ion + electron) are then described by the following terms:

$$[\text{In}^+(5s^2)^1S_0 + e^-(\epsilon s_{1/2})]_{J=1/2} \quad (4a)$$

$$[\text{In}^+(5s^2)^1S_0 + e^-(\epsilon d_{3/2})]_{J=3/2} \quad (4b)$$

Since the ionic core of indium has filled shells, i.e.  $L = S = J = 0$ , the total angular momentum of the final state  $J$  of the atomic system (ion + electron) is equal to the  $j$ -value of the outgoing photoelectron. Keeping in mind that

Table I. The photoionisation dynamical parameters, i.e. cross-section  $\sigma$ , angular asymmetry parameter  $\beta$ , and spin-polarisation parameters  $A$ ,  $\alpha$ , and  $\xi$ , as functions of reduced dipole-matrix elements  $D_{1/2}$ ,  $D_{3/2}$  and phase-shift difference  $\delta_{1/2} - \delta_{3/2}$  for  $\text{In}(5s^2 5p)^2 P_{1/2}$ .  $\alpha'$ ,  $a_0$  and  $\omega$  are the fine-structure constant, the Bohr radius and the photon energy in atomic units (1 a.u. = 2 Ry) respectively [19, 20]

$$\sigma = \sigma_{s_{1/2}} + \sigma_{d_{3/2}} = 4\pi^2 \alpha' a_0 \omega (D_{1/2}^2 + D_{3/2}^2) \quad (1)$$

$$\beta = \frac{D_{3/2}^2 + 2\sqrt{2}D_{3/2}D_{1/2} \cos(\delta_{1/2} - \delta_{3/2})}{D_{1/2}^2 + D_{3/2}^2} \quad (2)$$

$$A = \frac{D_{1/2}^2 - 0.5D_{3/2}^2}{D_{1/2}^2 + D_{3/2}^2} \quad (3)$$

$$\xi = \frac{3\sqrt{2}D_{1/2}D_{3/2} \sin(\delta_{1/2} - \delta_{3/2})}{4(D_{1/2}^2 + D_{3/2}^2)} \quad (4)$$

$$\alpha = \frac{-D_{3/2}^2 + \sqrt{2}D_{1/2}D_{3/2} \cos(\delta_{1/2} - \delta_{3/2})}{D_{1/2}^2 + D_{3/2}^2} \quad (5)$$

the decay of an autoionising state is determined by the  $J$ ,  $m_j$ -conservation (i.e.,  $\Delta J = \Delta m_j = 0$ ) it can take place only into one of the orthogonal electron continua:  $\varepsilon s_{1/2}$  or  $\varepsilon d_{3/2}$ .

As seen by Fig. 1(a), the photoionisation cross-section of the autoionising states are typically two or three orders of magnitude larger than the non-resonant cross section. Thus the photoionisation process in each resonance is dominated by the resonant dipole-matrix element  $D_{1/2}$  or  $D_{3/2}$  according to the final states involved [eq. 4(a, b)]. Theoretically, the photoionisation process of  $p_{1/2}$ -electrons is described by the energy dependence of two (complex) dipole-matrix elements  $D_{1/2}$  and  $D_{3/2}$  and the corresponding phase shift difference  $\Delta = (\delta_{1/2} - \delta_{3/2})$  [19, 20]. The dependence of the dynamical photoionisation parameters  $\sigma$ ,  $A$ ,  $\xi$ ,  $\alpha$  and  $\beta$  upon these quantities is given in Table I [19, 20].

Since the spin-polarisation parameter  $A$  [Table I, eq. (3)] is determined only by the ratio of the square of the dipole-matrix elements  $D_{1/2}$  and  $D_{3/2}$ , the sign of the experimental results of the parameter  $A$  allows to decide which electron continuum is enhanced in the resonance considered. Assuming that  $D_{1/2} \gg D_{3/2}$  or  $D_{3/2} \gg D_{1/2}$  one finds as limiting values for the spin polarisation parameter  $A$ :

$$A \rightarrow +1.0 \quad \text{or} \quad A \rightarrow -0.5, \quad \text{respectively.} \quad (5)$$

Since  $A$  is restricted to lie between  $-0.5$  and  $+1.0$  the resonance structure of this spin-polarisation parameter is in general broader than that of the intensity spectrum [23].

Figure 2 shows the spectral dependence of the experimental data for the spin-polarisation parameters  $A$ ,  $\xi$  and  $\alpha$  together with the cross-section for  $\text{In}(5s^2 5p)^2 P_{1/2}$ . The results for the spin-polarisation  $A$  clearly support the assignments of the autoionisation resonances (HF calculations of Connerade *et al.* [10]) since the two resonances with  $J = 1/2$  show high positive  $A$ -values and the two resonances with  $J = 3/2$  show negative  $A$ -values.

On the right wing of the  $\text{In}(5s5p^2)^2 P_{3/2}$  resonance one observes that the measured polarisation values  $A$  rise (Fig. 2) and then fall again to more negative values. This can be understood by the interpretation of Fano's formula (Fano [21]) for the simplest case; the interaction of an isolated discrete atomic level with a single continuum:

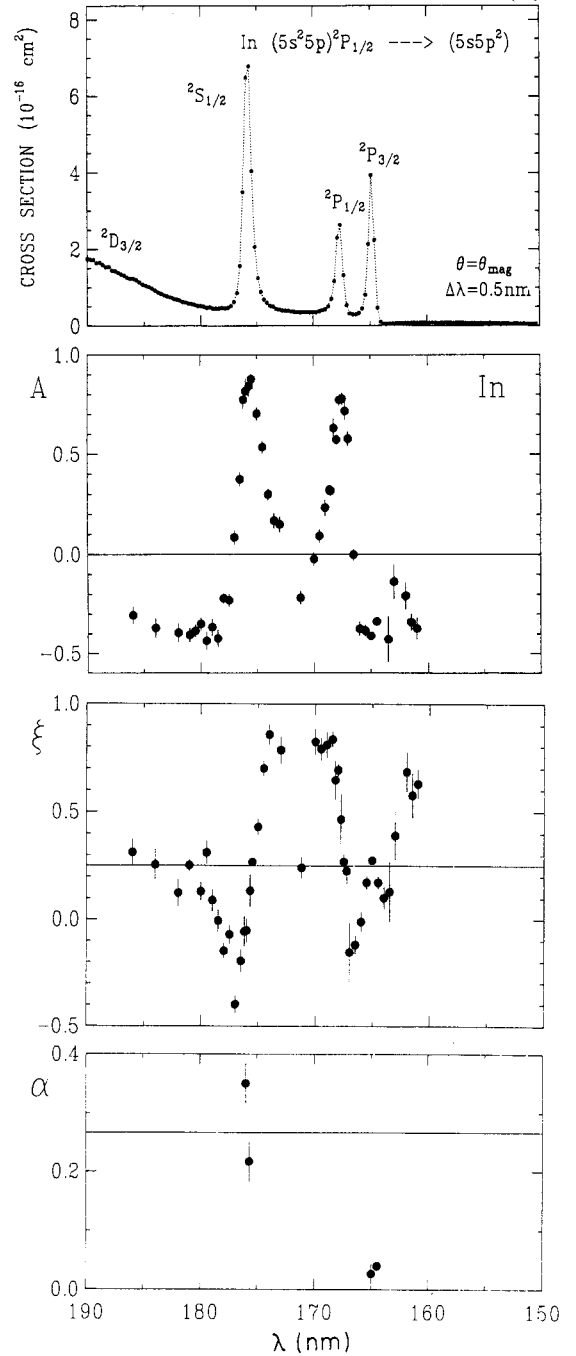


Fig. 2. Experimental results (full points with error bars) of the spin-polarisation parameters  $A$ ,  $\xi$  and  $\alpha$  for  $\text{In}(5s^2 5p)^2 P_{1/2}$  in the  $5s5p^2$ -autoionisation region together with the photoionisation cross section.

$$\sigma = \sigma_a \frac{(q + \varepsilon)^2}{(1 + \varepsilon^2)} + \sigma_b, \quad (6)$$

where  $\sigma_a$  and  $\sigma_b$  are the interacting and non-interacting part of the photoionisation cross section; the line shape parameters  $q$  and the energy parameter  $\varepsilon$  follow definition given by Fano [21]. Since  $q$  does not depend upon the photon energy, from eq. (6) it follows that at  $q = -\varepsilon$  the resonant contribution vanishes.

In the case of the  $\text{In}(5s5p^2)^2 P_{3/2}$ -resonance, this cross-section minimum (see Fig. 2) is obviously on the right wing of the resonance peak (also observed by Karamatskos *et al.* [11]). Since this resonance interacts only with the  $\varepsilon d_{3/2}$ -continuum we have here the special case of a minimum (possibly a zero) in one of the partial continua, here  $\varepsilon d_{3/2}$ .

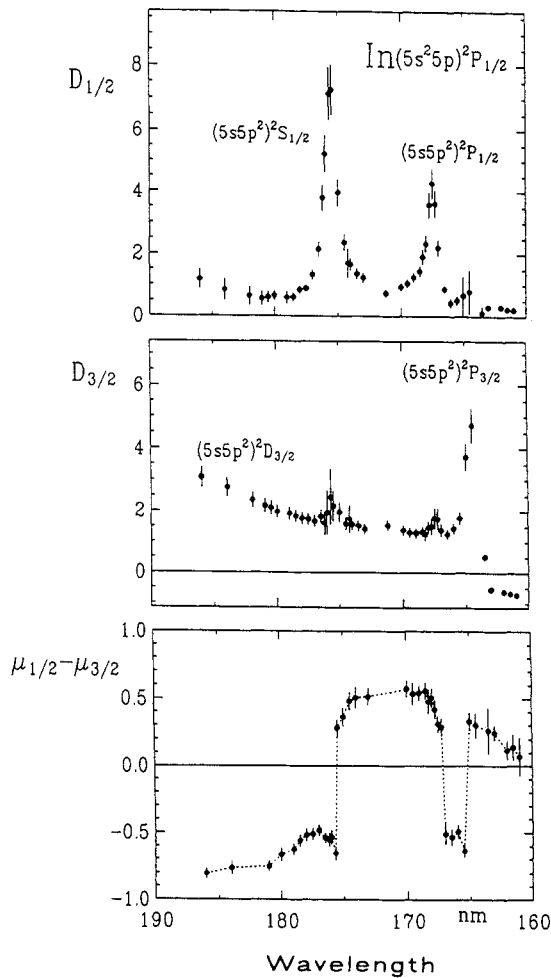


Fig. 3. Matrix elements  $D_{1/2}$ ,  $D_{3/2}$  and quantum defect difference  $\mu_{1/2} - \mu_{3/2}$  for photoionisation of In with final ionic state  $\text{In}^+(5s^2)^1S_0$  in the autoionisation region of the  $5s5p^2$ -configuration. The classification of the autoionisation resonances is indicated in the figures. The dotted line in the figure for the quantum defect difference  $\mu_{1/2} - \mu_{3/2}$  is the connection of points to guide the eyes.

Consequently, the  $\varepsilon S_{1/2}$ -continuum is dominating in this region and so the spin-polarisation  $A$  tends towards positive values [see Table I, eq. (3)]. The measured values for the  $\xi$ -parameter provide the possibility of a zero in the resonant partial cross section  $\varepsilon d_{3/2}$ , since in the vicinity of the cross section minimum the values for the  $\xi$ -parameter are close to zero and show a sign change. From eq. (4), Table I, this can be understood by a sign change of the resonant matrix element  $D_{3/2}$ .

Another important property of the  $\xi$ -parameter is its proportionality to the sine of the phase-shift difference  $\delta_{1/2} - \delta_{3/2}$ , [see eq. (4), Table I]. Therefore, a variation of the phase-shift difference is seen directly via the  $\xi$ -parameter. According to the theory of Fano [21], in each autoionisation resonance an increase by  $\pi$  of the phase-shift difference  $\delta_{1/2} - \delta_{3/2}$  should occur. The strong variation of the measured  $\xi$ -parameters in each resonance establishes this fact, best seen by the  $^2S_{1/2}$ - and  $^2P_{1/2}$ -resonance, where a pronounced change from negative to positive values and vice versa occurs.

From the angular dependence of  $A(\Theta)$  [see eq. (1a)] we have determined the  $\alpha$ -parameter in the vicinity of the resonance maxima of the  $^2S_{1/2}$ - and  $^2P_{1/2}$ -resonance. In the range of the  $^2S_{1/2}$ -resonance the  $\alpha$ -values are small  $|\alpha| \sim 0.2$  reflecting the dominance of the matrix element  $D_{1/2}$  (see eq. (5), Table

I), whereas in the case of the  $^2P_{3/2}$ -resonance ( $D_{3/2}$ -matrix element dominates) high negative values are observed.

From the experimental data for  $\sigma$ ,  $A$ ,  $\alpha$  and  $\xi$  the three unknown quantities  $D_{1/2}$ ,  $D_{3/2}$  and  $\delta_{1/2} - \delta_{3/2}$  have been determined by use of the analytical dependence given in Table I. Since for this system (ion and electron) three suitably measured parameters are already sufficient to determine the matrix elements and the phase-shift differences, the other two dynamical parameters check the consistency of the experimental data. The results of our evaluation are shown in Fig. 3 as function of photon wavelength. We have plotted the quantum-defect difference  $\mu_{1/2} - \mu_{3/2}$  as measure for the phase-shift difference, i.e., we have subtracted the Coulomb phase. The relation of the quantum defect  $\mu_i$  to the phase shift  $\delta_i$  is given by the following equation:

$$\delta_i = \sigma_i + \pi\mu_i - \pi(l/2), \quad (7)$$

where  $\sigma_l$  is the Coulomb phase-shift for an outgoing partial wave with angular momentum  $l$  in a pure Coulomb field. Deviations from the Coulomb field are characterized by the additional phase-shift  $\pi\mu_i$ ; the term  $\pi(l/2)$  satisfies the sign convention of the matrix elements.

The matrix elements evaluated show for the  $^2S_{1/2}$ -,  $^2P_{1/2}$ - and the  $^2P_{3/2}$ -states a resonance behaviour for the  $D_{1/2}$ - or the  $D_{3/2}$ -matrix elements, respectively. Similar to the  $A$ -parameter, the width of the structures are broader for the  $D_{1/2}$ - or  $D_{3/2}$ -matrix elements than in the cross section. Further these data reflect clearly the asymmetry of the line shapes of the resonances; in particular the  $^2S_{1/2}$ - and the  $^2P_{1/2}$ -resonance have asymmetries of different signs (not seen as clearly in the cross section).

For the  $^2S_{1/2}$ -,  $^2P_{1/2}$ - and  $^2P_{3/2}$ -resonance one can see that the matrix elements of the “wrong”-channel rise; we attribute this to the evaluation procedure of  $D_i$ , neglecting effects resulting from the radiation bandwidth of  $\Delta\lambda = 0.5$  nm. The wavelength dependence of the  $D_{3/2}$ -matrix elements illustrates the dominance of the broad  $^2D_{3/2}$ -autoionisation resonance in the wavelength range investigated. It is clearly shown, that for the  $\varepsilon d_{3/2}$ -continuum one needs to take into account the procedure to handle non-isolated overlapping resonance structures according to Mies [22], since the  $^2P_{3/2}$ -resonance is situated in the wing of the  $^2D_{3/2}$ -resonance.

The quantum defect difference  $\mu_{1/2} - \mu_{3/2}$  evaluated shows a rapid variation in each autoionisation resonance. The differences  $\Delta = |\mu_{1/2} - \mu_{3/2}|$  is close to 1 according to a phase variation of  $\pi$  as predicted by the theory of Fano [21].

Concluding, in the present investigation a complete quantum-mechanical characterization of the photoionisation process of the open shell atom  $\text{In}(5s^25p)^2P_{1/2}$  in the autoionisation region of the  $(5s5p^2)$  levels is given. Dipole-matrix elements and phase-shift differences were determined from the measured values of the photoelectron spin-polarisation parameters  $A$ ,  $\xi$ ,  $\alpha$  and the photoionisation cross section. The experimental data confirm the classification of the resonances given by Connerade *et al.* [10].

#### Acknowledgement

Our thanks are due to the BESSY staff for useful cooperation. Technical help and discussions with H. W. Klausung, M. Salzmann, Dr A. Svensson, Dr Ch. Heckenkamp and Prof. Cherepkov are gratefully acknowledged. Support from the Bundesministerium für Forschung und Technologie (05331 and 431 AX) is gratefully acknowledged.

**References**

1. Heinzmann, U., *J. Phys. B: At. Mol. Phys.* **13**, 4353 (1980).
2. Heinzmann, U., *J. Phys. B: At. Mol. Phys.* **13**, 4367 (1980).
3. Schäfers, F., Schönhense, G. and Heinzmann, U., *Z. Phys.* **A304**, 41 (1982).
4. Schönhense, G., Schäfers, F., Heckenkamp, Ch. and Heinzmann, U., *J. Phys. B: At. Mol. Phys.* **17**, L771 (1984).
5. Heckenkamp, Ch., Schäfers, F., Schönhense, G. and Heinzmann, U., *Z. Phys.* **D2**, 257 (1986).
6. Garton, W. R. S., *Proc. Phys. Soc.* **65**, 864 (1954).
7. Garton, W. R. S., Parkinson, W. H. and Reeves, E. M., *Can. J. Phys.* **44**, 1745 (1966).
8. Marr, G. V. and Heppingstall, R., *Proc. Phys. Soc.* **87**, 293 (1966).
9. Kozlov, M. G. and Startsev, G. P., *Opt. Spectros.* **24**, 3 (1968).
10. Connerade, J. P. and Baig, M. A., *J. Phys. B: At. Mol. Phys.* **14**, 29 (1981).
11. Karamatskos, N., Müller, M., Schmidt, M. and Zimmerman, P., *J. Phys. B: At. Mol. Phys.* **17**, L341 (1984).
12. Heinzmann, U., Heuer, H. and Kessler, J., *Phys. Rev. Lett.* **34**, 441 (1975).
13. Cherepkov, N. A., *J. Phys. B: At. Mol. Phys.* **13**, L181 (1980).
14. Cherepkov, N. A., *Adv. At. Mol. Phys.* **19**, 395 (1983).
15. Fano, U., *Phys. Rev.* **178**, 131 (1969).
16. Heinzmann, U., *Phys. Scripta* **T17**, 77 (1987) (and references therein).
17. Heckenkamp, Ch., Evers, A., Schäfers, F., Schönhense, G. and Heinzmann, U., *Nucl. Instr. Methods* **A246**, 500 (1986).
18. Schäfers, F., Peatman, W., Evers, A., Heckenkamp, Ch., Schönhense, G. and Heinzmann, U., *Rev. Sci. Instrum.* **57**, 1032 (1986).
19. Huang, K. N., *Phys. Rev.* **A22**, 223 (1980).
20. Cherepkov, N. A., *J. Phys. B: At. Mol. Phys.* **12**, 1279 (1979).
21. Fano, U., *Phys. Rev.* **124**, 1866 (1961).
22. Mies, F. H., *Phys. Rev.* **175**, 164 (1968).
23. Heinzmann, U. and Kessler, J., *J. Phys. B: At. Mol. Phys.* **11**, L265 (1978).